

PERMEABILITY STUDIES ON A SILICALITE SINGLE CRYSTAL MEMBRANE MODEL

E.R. Geus¹, A.E. Jansen², J.C. Jansen¹, J. Schoonman¹, and H. van Bekkum¹
¹ Delft University of Technology, Laboratory of Applied Chemistry,
Julianalaan 136, 2628 BL Delft, The Netherlands
² TNO-MT, Utrechtseweg 48, 3704 HE Zeist, The Netherlands

SUMMARY

Permeation experiments on large silicalite single crystals (MFI type), embedded in an epoxy resin were performed, using permanent gases and small alkanes. A scaling-up from initially a one zeolite crystal membrane to a multi zeolite crystal membrane is presented. Differences in permeability were small and attributed to a sorption-diffusion mechanism, in qualitative agreement with theory. As permeation may vary within different regimes, maximum selectivities are expected in the Henry region. Some boundary conditions in the preparation of (ceramic) zeolite membranes are formulated.

INTRODUCTION

Zeolite membranes may open new horizons in both separation technology and reaction engineering. At present, most gas separation membrane processes are operated using polymer membranes. Ceramic membranes can be used at higher temperatures, which allows regeneration and catalytic application (ref. 1). The sol-gel technique has been used successfully in the preparation of ceramic membranes (refs. 2-5). Alumina gas separation membranes can be produced on a semi-industrial scale with relative ease (ref. 6). Zeolite membranes in an all-ceramic system are expected to exhibit significantly higher selectivities due to the zeolite's molecular sieve characteristics.

In the development and use of zeolite membranes it is essential to obtain information on the mass transport through zeolite crystals. Recently an extensive mathematical model for the permeation through porous crystal membranes has been proposed by Barrer (ref. 7).

In the experimental field Hayhurst and Paravar (refs. 8-9) reported on the determination of the diffusivity of alkanes by means of a zeolite membrane configuration. These experiments, however, were performed on a twinned silicalite crystal at low feed pressures. Recently this work was extended by similar experiments on benzene passage through a silicalite single crystal (ref. 10). Wernick and Osterhuber (refs. 11-12) reported on the permeation through a NaX single crystal. Significantly higher feed pressures were used in these experiments, and the permeation characteristics in time were emphasized.

According to patent literature ceramic zeolite membranes have been prepared by crystallizing zeolites in situ either in (ref. 13), or on (refs. 14-18) a macroporous support. Alternatively, small zeolite crystallites together with

a ceramic binder are said to cover a macroporous support completely (ref. 19), or result in an unsupported film (ref. 20). Recently Bein et al. (ref. 21) reported on the preparation of inorganic thin films, containing zeolite crystals (type Y and chabazite).

In the above cited patent literature it is emphasized that the size of the zeolite crystals (i.e. the membrane thickness) should be minimized to realize sufficiently high permeabilities. On the other hand, large zeolite crystals are expected to be most practical in the preparation of zeolite membranes (ref. 22), and in the authors' opinion especially on a laboratory scale.

In this work the permeation of permanent gases and linear alkanes through silicalite single crystals in a membrane configuration has been subjected to a first scaling-up. To that end several crystals were embedded into an epoxy resin matrix on a perforated metal layer, preliminary to all-ceramic membranes which are in preparation.

This study also intends to improve knowledge on (i) pitfalls in the preparation of zeolite membranes, and (ii) the operation under practical conditions (e.g. high feed pressures). In addition, unexpected behaviour of zeolite membranes (caused by e.g. cracking of zeolite crystals or fouling) could be diagnosed.

THEORY

Barrer (ref. 7) recently proposed a permeation model for systems obeying Langmuir's isotherm in which activated intracrystalline diffusion takes place. In addition external surface effects on both feed and permeate side were included, resulting in a five step process. In this work we will focus on the overall permeability, which is expected to be governed by a sorption-diffusion mechanism.

A convenient way to define the permeation rate of a membrane makes use of the permeability (ϕ) (ref. 23), which can be derived from Fick's first law of diffusion:

$$\Phi_{\text{mol}} = \phi * A_m / l_m * \Delta p \quad [1]$$

in which Φ_{mol} denotes the steady state flow, A_m the surface area of the membrane, l_m the membrane thickness (in this work the crystal size in the b-direction), and Δp the pressure difference over the membrane. The permeability should be considered a phenomenological parameter of the membrane, resulting from specific conditions (i.e. pressure, temperature, feed composition, degree of fouling). Formula [1] will be used to calculate the permeability from the permeation rate at steady state.

According to Barrer's model, maximum permeation will occur when the mass transport is only governed by intracrystalline diffusion. This holds if sorption processes on both sides of the membrane are much faster than

intracrystalline diffusion:

$$\Phi_{\text{mol,max}} = D_{\text{intra,diff}} * A_m/l_m * \Delta c^{\text{max}} \quad [2]$$

in which Δc^{max} denotes the maximum concentration difference over the membrane. Δc^{max} can be derived from sorption isotherms (assuming equilibrium between gas and adsorbed phase). $D_{\text{intra,diff}}$ can be obtained from NMR data, referring to the intracrystalline self-diffusivity (D_{self}). The PFG NMR technique measures D_{self} directly, albeit only for rapid processes (ref. 24). The Darken equation enables one to calculate the intracrystalline Fickian diffusivity (ref. 25):

$$D_{\text{intra,diff}} = D_{\text{self}} * \partial \ln p / \partial \ln c \quad [3]$$

For the Langmuir isotherm, equation [3] may be written as:

$$D_{\text{intra,diff}} = D_{\text{self}} * 1/(1 - \theta) \quad [4]$$

in which θ denotes the fraction of sites occupied. NMR results (ref. 26) have shown that for small alkanes (C_1 - C_3) D_{self} decreases for increasing carbon number, due to the diminished molecular free volume. For sufficiently high θ , this effect is overruled by the increase of $1/(1 - \theta)$ (ref. 25).

During permeation a concentration profile will exist over the zeolite crystals, which will remain constant at steady state. As θ varies over the membrane, an average diffusivity can be found by integrating over the total membrane. Finally, equation [2] is rewritten as:

$$\Phi_{\text{mol,max}} = \{D_{\text{intra,diff}}\}^{\text{av}} * A_m/l_m * \Delta c^{\text{max}} \quad [5]$$

When θ is high over the whole membrane, the Fickian $D_{\text{intra,diff}}$ will be significantly higher than the NMR D_{self} . Thus, the sorption equilibrium will influence the permeability of a species, and both sorption and diffusion should be considered in evaluating the permeability through a zeolite membrane.

EXPERIMENTAL

Large, flat silicalite single crystals were synthesized as described by Jansen et al. (ref. 27). The Si/Al ratio (> 300) was determined by ICP analysis on large crystals from a single batch. Selected crystals of about equal size ($a, b, c = 200 * 100 * 350 \mu\text{m}$) were carefully calcined at 500°C (heating rate 1°C/min).

In a preliminary experiment one large silicalite crystal was mounted in an epoxy resin film (bisphenol A glycidyl ether/poly amine; Araldit, Ciba-Geigy). As this procedure was rather time consuming and complex, a more

practical procedure was developed.

Thin copper platelets (thickness 50 μm) were provided with up to 20 holes (diameter 150 μm). Any remaining oil was removed by cleaning the plate in boiling acetone, and drying in air. The components of the epoxy resin were homogeneously mixed and carefully spread around each hole. A silicalite single crystal was positioned on each hole. The epoxy resin showed good adhesion towards both the zeolite surface and the copper. The starting viscosity of the epoxy upon mixing is very low. This resulted in an epoxy film over the total crystal surface facing the copper plate (b-direction).

After 1-2 hours, the viscosity of the epoxy had increased strongly. The adhesion to the zeolite material is still excellent. Therefore, the zeolite crystals are preferably placed on the platelet at this stage of the hardening of the epoxy resin. The epoxy resin had hardened within 24 hours completely. Table 1 gives characteristics of the various membranes.

TABLE 1: Zeolite-epoxy-on copper composites studied in this work

Code	$N^{\&}$	$A_m^{\%}$ (m^2)	l_m (m)	Remarks
M1	0	$1.2 \cdot 10^{-5}$	$1.0 \cdot 10^{-4}$	epoxy resin film in a perforated platelet
C1	1	$1.68 \cdot 10^{-8}$	$9.0 \cdot 10^{-5}$	as-synthesized single crystal, containing Pr_4N^+ template
MES-Z1	1	$3.0 \cdot 10^{-8}$	$1.0 \cdot 10^{-4}$	initial preparation method
5ZH-1	5	$4.48 \cdot 10^{-8}$	$1.0 \cdot 10^{-4}$	measurements at 30° and 120° C
LPZ-1	10	$1.36 \cdot 10^{-7}$	$9.0 \cdot 10^{-5}$	measurements at 30° C
LPZ-3a,b,c	8	$1.10 \cdot 10^{-7}$	$9.0 \cdot 10^{-5}$	sequence of measurements at 30°, 130°, and 30° C; LPZ-1 after repair

$\&$) number of crystals embedded

$\%$) effective surface area, determined by light microscopy

Figure 1 shows an embedded zeolite crystal in epoxy on a copper plate. The zeolite membranes were inspected by means of light microscopy. Figure 2 demonstrates the determination of the effective surface area of an embedded zeolite crystal. In addition, the integrity of each embedded zeolite crystal was checked by microscope FTIR-spectroscopy.

The experimental set-up is described elsewhere (ref. 28). Permanent gases (H_2 (99.5%), N_2 (99.999%), and O_2 (99.995%)), small alkanes (methane (99.5%), ethane (99.9%), and n-butane (99.0%)), and carbon dioxide (99.7%) were used as permeate feeds. Measurements were performed at permeation periods of 2-10 minutes. Feed pressures were within 1-2 bar. Permeate pressures always started at approximately 2-4 Pa, and never exceeded 100 Pa, except for hydrogen (< 250 Pa). As some inleak occurred (approximately 0.01 Pa/s) permeation rates could not be determined at too low a pressure rise. By embedding several silicalite crystals in one membrane the accuracy of the measurements was increased.

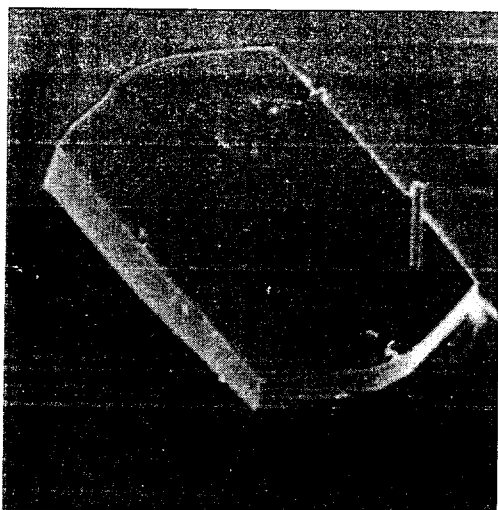


Fig. 1. Silicalite crystal, embedded in epoxy resin



Fig. 2. Determination of free area (lighter area in the centre of the zeolite crystal)

RESULTS

Some preliminary experiments were performed as to make sure that only transport through the zeolite crystals was to take place. To double check, experiments were carried out several times, using different membranes.

The non-permeability of the epoxy resin was checked by membrane M1. Up to 200° C no permeation could be detected, establishing that the epoxy resin meets the requirements.

On an as-synthesized crystal (still containing the template molecules; membrane C1), embedded in a similar way, no permeation could be detected. The expected permeation rate (related from measurements on LPZ-3b at similar conditions) should have been significantly higher than the accuracy of the apparatus. Thus, it was concluded that zeolite crystals could be embedded properly by means of the present procedure.

Membrane MES-Z1 is the initial one crystal composite. For all gases very high permeabilities were found (cf. Table 2), resulting in Knudsen diffusion selectivity. Inspection by scanning electron microscopy revealed a large crack in the zeolite crystal. The high permeability and Knudsen selectivity are attributed to the presence of this crack.

Permeation results on membrane LPZ-1 are listed in Table 2 as well. The permeability for each gas seemed to increase slightly after repeated experiments. For this reason LPZ-1 was removed from the cell for inspection. Two out of ten crystals appeared to be cracked, and subsequently these crystals were completely covered by fresh epoxy resin.

Permeation rates through the thus repaired membrane (LPZ-3; Figure 3) were

nearly two orders of magnitude lower than for LPZ-1 (cf. Table 2). This change in permeability can not be accounted for by the loss of free surface area, which is only 20%. It can be seen from Table 2 that no high selectivities for the various gases were found. The permeability for n-butane at 30° C (LPZ-3a) was higher than for other gases tested.

TABLE 2: Experimental permeabilities for permanent gases and alkanes on zeolite-epoxy composites

Membrane	MES-Z1	Permeability (nmol.m/m ² .s.Pa)			
		LPZ-1	LPZ-3a	LPZ-3b	LPZ-3c
T (°C)	25	30	30	130	30
Δp (bar)	1-2	1.6-1.8	1.6	1.6	1.6
Gas					
H ₂	780	0.69	0.0095	0.0234	0.0430
N ₂	170	0.24	0.0046	0.0058	0.0134
O ₂	200	0.33		0.0057	0.0120
CO ₂	170	0.20		0.0052	
CH ₄	250	0.32	0.0037	0.0082	0.0182
C ₂ H ₆		0.37	0.0027	0.0065	0.0158
n-C ₄ H ₁₀	120	0.42	0.0145	0.0056	

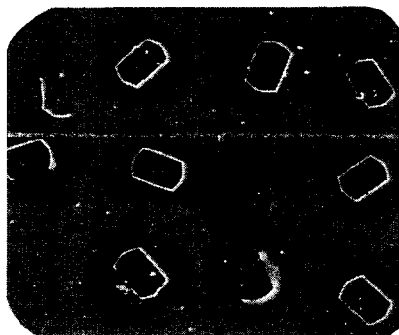


Fig. 3. Membrane LPZ-3; the two cracked crystals are completely covered by epoxy resin

As the temperature was raised to 130° C (LPZ-3b), permeabilities of all gases slightly increased, except for n-butane (decrease of 70%). Again, selectivities were found to be rather small. The measurements on LPZ-3a and LPZ-3b were highly reproducible.

Upon cooling to 30° C (LPZ-3c) again, all permeabilities were found to be much higher compared to LPZ-3a. In contrast to the previous experiments, these experiments were not very reproducible. Upon inspection it was indeed

found that some crystals were cracked, so the increased permeability is not an effect of the activation at higher temperature.

During the first few experiments on LPZ-3a (at 30° C) the zeolite pores proved to be obstructed by adsorbed water. FTIR-spectra (Figure 4) of calcined silicalite crystals reveal a considerable amount of adsorbed water under ambient conditions. As the phenomenon vanished after some experiments, the adsorbed water is apparently induced to desorb by the permeating gas.

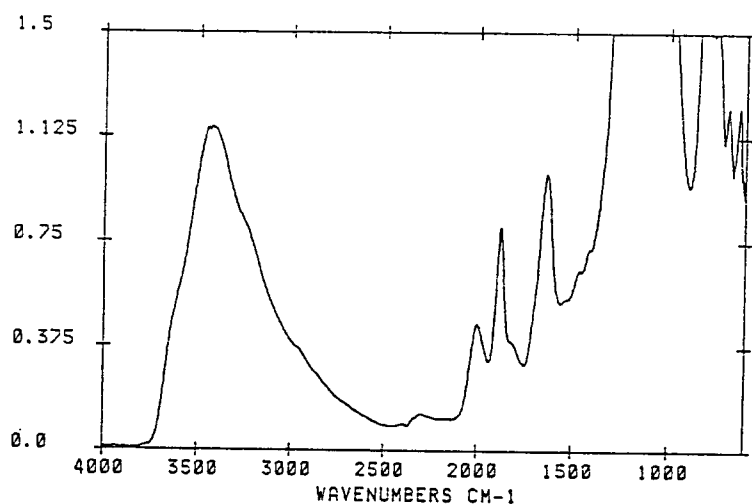


Fig. 4. FTIR-spectrum of embedded silicalite crystal

The above-mentioned phenomenon was also observed during experiments on membrane 5ZH-1 at room temperature. Only few experiments were performed at 30° C, after which the temperature was raised to 90° C. The permeability decreased at this high temperature, and finally the membrane was completely impermeable. Inspection of the zeolite crystals by microscope FTIR-spectroscopy revealed C-H-vibrations (Figure 5). As these vibrations do not refer to the zeolite framework it was concluded that some obstructing guest molecule was stabilized within the zeolite framework at high temperature.

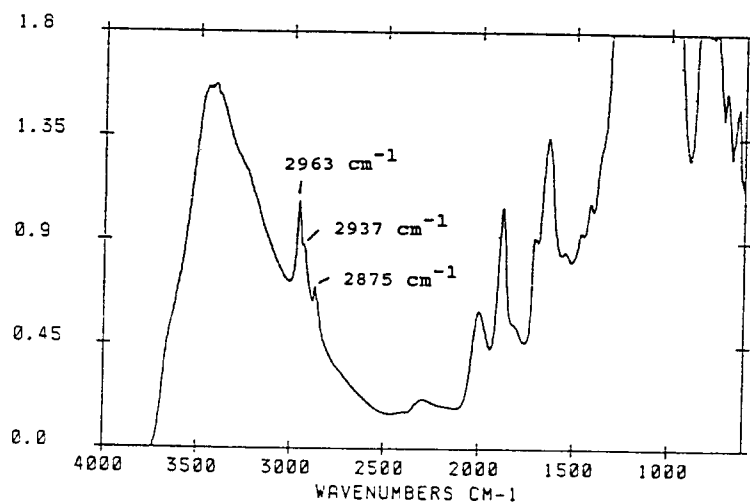


Fig. 5. FTIR-spectrum of non-permeable silicalite crystal due to fouling

DISCUSSION

In Table 3 the calculation of the maximum flow according to equation [5] is shown for the linear alkanes C_1 - C_4 at 30° , assuming a linear concentration profile. Unfortunately, the required data on sorption (ref. 29) and diffusion (ref. 26) were rather incomplete. The effect of sorption on $D_{\text{Fick}}^{\text{av}}$ is only demonstrated qualitatively.

TABLE 3: Maximum theoretical flows of linear alkanes C_1 - C_4 for membrane LPZ-3, calculated from equation [5]

T = 30° C; Δp = 1.5 bar; pressure on permeate side: 100 Pa							
gas	Δc^{max} (mol/m ³)	θ_F % (-)	θ_P % (-)	$D_{\text{self}}^{\text{max}}$ (m ² /s)	$D_{\text{Fick}}^{\text{av}}$ (m ² /s)	$\Phi_{\text{mol,max}}$ (pmol/s)	ϕ (mol.m/m ² .s.Pa)
CH ₄ §	3600	0.63	0.00	$1.2 \cdot 10^{-8}$	$1.48 \cdot 10^{-8}$	65.3	$3.56 \cdot 10^{-10}$
C ₂ H ₆	3472	0.67	0.02	$7.5 \cdot 10^{-9}$	$5.01 \cdot 10^{-9}$	21.2	$1.16 \cdot 10^{-10}$
C ₃ H ₈	3154	0.81	0.07	$6.0 \cdot 10^{-10}$	$4.14 \cdot 10^{-9}$	16.0	$8.71 \cdot 10^{-11}$
C ₄ H ₁₀ #	1083	0.83	0.53	$5.0 \cdot 10^{-11}$	$6.31 \cdot 10^{-10}$	0.84	$4.55 \cdot 10^{-12}$

%) fraction of sites occupied on feed (F) and permeate (P) side (equilibrium)

§) data extrapolated from sorption data (ref. 29), cf. text

#) data extrapolated from diffusion data (ref. 26), cf. text

The intracrystalline self-diffusivity of n-butane can not be determined by the PFG NMR technique (ref. 30), and was estimated from data on methane, ethane, and propane. The correlation of the intracrystalline diffusivity to the carbon number for n-alkanes, found by Eic and Ruthven with the ZLC method (ref. 30) was used. The sorption data on methane were estimated from sorption isotherms of ethane, propane, and n-butane (ref. 29).

Because of lack of sufficient data, permeabilities of permanent gases (H_2 , N_2 , and O_2) and carbon dioxide were not calculated. The sorption behaviour of nitrogen and to a lesser extent carbon dioxide has been shown (ref. 31) to obey Henry's law up to high temperatures (70° C), and high pressures (up to 1 bar). In contrast to the alkanes, no sorption effect is expected for permanent gases, as $(\partial \ln p / \partial \ln c)$ remains constant.

In contrast to theory (Table 3), small differences in permeability are measured (Table 2). Permeabilities are considerably smaller (methane, ethane) than the maximum flows, or of the same magnitude (n-butane). This implicates that other processes (e.g. sorption to and from the zeolite pores) than intracrystalline diffusion govern the permeation.

Applying low feed pressures (up to 1.8 kPa), Hayhurst and Paravar have found high selectivities (ref. 9). In their experiments however, permeation occurred through the c-direction (ref. 32), resulting in a high tortuosity factor. Permeation may therefore be hindered, especially for higher alkanes.

Negligible selectivity was also found by Wernick and Osterhuber (ref. 11) on binary and ternary mixtures of various alkanes (NaX crystal). The reported

rapid and slow permeation regime transition may be (partly) explained by the sorption effect on intracrystalline diffusion, as high feed pressures (1 bar) were applied (permeate pressure < 133 Pa). In the rapid permeation regime the factor ($\partial \ln p / \partial \ln c$) will be high, due to high site occupation. This rapid regime was found to be metastable for higher temperatures (65°-100° C). Sorption experiments by Stach et al. (ref. 33) have shown that sorption on permeate side (13.3-133 Pa) decreases strongly in this temperature region.

From these studies it is concluded that the highest selectivities will be realized in the Henry regime. Table 3 indicates that at equal conditions the difference between $D_{\text{self}}^{\text{max}}$ and $D_{\text{Fick}}^{\text{av}}$ will be larger for higher alkanes. As sorption is small in the Henry region, the permeation is governed by the intrinsic diffusivity only. In order to achieve high permeabilities, the Henry regime is favourably reached by an increase of temperature.

CONCLUSION

Large silicalite single crystals have been found to be permeable for permanent gases and small alkanes. A scaling-up of the mass transfer was achieved by embedding several zeolite crystals into one membrane.

Permeation through zeolite membranes may occur within different regimes. Maximum selectivity is expected to be realized in the Henry region, in which the intracrystalline diffusivity is hardly affected by sorption.

The application of large zeolite crystals in preparing zeolite membranes is to be preferred from a preparative point of view. Draw-backs, however, may be the sensitivity to high feed pressures, and relatively low permeabilities. As zeolite membranes have to be (re)-activated, all-ceramic membrane configurations are strongly recommended.

ACKNOWLEDGEMENT

E.R. Geus is very grateful to Prof. R.M. Barrer for a stimulating discussion on zeolites as membranes.

REFERENCES

- 1 H.P. Hsieh, Inorganic Membrane Reactors - A Review, AIChE Symposium Series 5, 85, no. 268, (1989), 53-67;
- 2 A. Larbot, A. Julbe, C. Guizard, L. Cot, J.Membr.Sci., 93, (1989), 289-303;
- 3 A. Larbot, J.P. Fabre, C. Guizard, L. Cot, J.Am.Ceram.Soc., 72, (1989), 257-61;
- 4 W.A. Zeltner, M.A. Anderson, 'Chemical Control over Ceramic Membrane Processing: Promises, Problems and Prospects', in: Proc. 1st Int.Conf.Inorg.Membr., (eds. J. Charpin, L. Cot), Montpellier, France, July 3-6, 1989, 213-223;
- 5 A. Leenaars, Preparation, Structure and Separation Characteristics of Ceramic Alumina Membranes, thesis, University of Twente, Netherlands, (1984);
- 6 H.M. van Veen, R.A. Terpstra, J.P.B.M. Tol, H.J. Veringa, 'Three-Layer Ceramic Alumina Membrane for High Temperature Gas Separation Applications', in: Proc. 1st Int.Conf.Inorg.Membr., (eds. J. Charpin, L. Cot), Montpellier, France July 3-6, 1989, 329-335;

- 7 R.M. Barrer, *J.Chem.Soc.Faraday Trans.*, 86(7), (1990), 1123-1130;
- 8 A.R. Paravar, D.T. Hayhurst, 'Direct Measurement of Diffusivity for Butane Across a Single Large Silicalite Crystal', 6th Int.Zeol.Conf., (Eds. D. Olson, A. Bisio), Reno, USA, July 10-15, 1983, 217-224;
- 9 D.T. Hayhurst, A.R. Paravar, *Zeolites*, 8, (1988), 27-29;
- 10 V.V. Nesarikar, D.B. Shah, D.T. Hayhurst, poster on BZA meeting, Chislehurst, England, July 15-20, 1990;
- 11 D.L. Wernick, E.J. Osterhuber, 'Diffusional Transition in Zeolite NaX: 1. Single Crystal Gas Permeation Studies', 6th Int.Zeol.Conf., (Eds. D. Olson, A. Bisio), Reno, USA, July 10-15, 1983, 122-130;
- 12 D.L. Wernick, E.J. Osterhuber, *J.Membr.Sci.*, 22, (1985), 137-146;
- 13 H. Suzuki, European Patent Application 180,200, (1985) to H. Suzuki;
- 14 M. Oyama, Japanese Patent 63,291,809, (1988) to Idemitsu Kosan Co.Ltd.;
- 15 H. Suzuki, US Patent 4,699,892, (1987) to H. Suzuki;
- 16 I.M. Lachman, M.D. Patil, US Patent 4,800,187, (1989) to Corning Glass Works;
- 17 H. Suzuki, European Patent Application 135,069, (1986) to H. Suzuki;
- 18 S. Satoshi, N. Tagaya, T. Maeshima, T. Isoda, Canadian Patent 1,235,684, (1988) to Toa Nenryo Kogyo Kabushiki Kaisha;
- 19 K. Miyazaki, Japanese Patent 60,129,119, (1985) to Matsushita Denki Sangyo K.K.;
- 20 G. Bellussi, F. Buonomo, A. Esposito, M. Clerici, U. Romano, European Patent Application 265,018 (1988) to Eniricerche, Snamprogetti, Enichem Synthesis;
- 21 T. Bein, K. Brown, C.J. Brinker, 'Molecular Sieve Films from Zeolite-Silica Microcomposites', *Stud.Surf.Sci.Catal.*, 49, (1989), 887-896;
- 22 U. Muller, A. Reich, K.K. Unger, *Stud.Surf.Sci.Catal.*, 52, (1989), 241-251;
- 23 K. Kammermeyer, *Gas and Vapor Separations by Means of Membranes, Progress in Separation and Purification, Vol. 1*, (Ed. E.S. Perry), Wiley, (1968), 335-372;
- 24 J. Kärger, D.M. Ruthven, *Zeolites*, 9, (1989), 267-281;
- 25 J. Kärger, S.P. Shdanov, A. Walter, *Z.phys.Chemie, Leipzig* 256, (1975), 319-329;
- 26 J. Caro, M. Bülow, W. Schirmer, J. Kärger, W. Heink, H. Pfeifer, S.P. Zdanov, *J.Chem.Soc.Faraday Trans.*, 81, (1985), 2541-2550;
- 27 J.C. Jansen, E. Biron, H. van Bekkum, *Stud.Surf.Sci.Catal.*, 37 (1988), 133-141;
- 28 H.C.W.M. Buys, A. van Elven, A.E. Jansen, A.H.A. Tinnemans, *J.Appl.Pol.Sci.*, in press;
- 29 R.E. Richards, L.V.C. Rees, *Langmuir*, 3, (1987), 335-340;
- 30 M. Eic, D.M. Ruthven, *Stud.Surf.Sci.Catal.*, 49, (1989), 897-905;
- 31 P. Graham, A.D. Hughes, L.V.C. Rees, *Gas Sep.Purif.*, 3, (1989), 56-64;
- 32 D.T. Hayhurst, private communication;
- 33 H. Stach, S.P. Shdanov, K. Fiedler, W. Schirmer, N.N. Samulevic, *Z.phys.Chemie, Leipzig*, 260, (1979), 455-464.